A $\sim$15 kpc outflow cone piercing through the halo of the blue compact dwarf galaxy SBS 0335-052E

Escape of Lyman radiation from galactic labyrinths
(Crete, April 18-21, 2023)

Edmund Christian Herenz

ESO Chile Fellow / Leiden Observatory

April 20, 2023

A&A 670, A121 (2023)
https://doi.org/10.1051/0004-6361/202244930

Astronomy & Astrophysics

A ~15 kpc outflow cone piercing through the halo of the blue compact metal-poor galaxy SBS 0335–052E★

E. C. Herenz[1,2], J. Inoue[3], H. Salas[4], B. Koenigs[3], C. Moya-Sierralta[5], J. M. Cannon[3], M. Hayes[6], P. Papaderos[7], G. Östlin[6], A. Bik[6], A. Le Reste[6], H. Kusakabe (日下部 晴香)[8], A. Monreal-Ibero[2], and J. Puschnig[9]

1 European Southern Observatory, Av. Alonso de Córdova 3107, 763 0355 Vitacura, Santiago, Chile
e-mail: eherenz@eso.org
2 Leiden Observatory, Leiden University, Niels Bohrweg 2, 2333 CA Leiden, The Netherlands
3 Department of Physics & Astronomy, Macalester College, 1600 Grand Avenue, Saint Paul, MN 55105, USA
4 Leibniz-Institut für Astrophysik Potsdam (AIP), An der Sternware 16, 14482 Potsdam, Germany
5 Pontificia Universidad Católica de Chile – Instituto de Astrofísica, Av. Vicuña Mackenna 4860, 897 0117 Macul, Santiago, Chile
6 Department of Astronomy, Stockholm University, AlbaNova University Centre, 106 91 Stockholm, Sweden
7 Instituto de Astrofísica e Ciências do Espaço – Centro de Astrofísica da Universidade do Porto, Rua das Estrelas, 4150-762 Porto, Portugal
8 Observatoire de Genève, Université de Genève, Chemin Pegasi 51, 1290 Versoix, Switzerland
9 Universität Bonn, Argelander-Institut für Astronomie, Auf dem Hügel 71, 53121 Bonn, Germany

Received 9 September 2022 / Accepted 5 December 2022

ABSTRACT

Context. Outflows from low-mass star-forming galaxies are a fundamental ingredient for models of galaxy evolution and cosmology. Despite seemingly favourable conditions for outflow formation in compact starbursting galaxies, convincing observational evidence for kiloparsec-scale outflows in such systems is scarce.

Aims. The onset of kiloparsec-scale ionised filaments in the halo of the metal-poor compact dwarf SBS 0335−052E was previously not linked to an outflow. In this paper we investigate whether these filaments provide evidence for an outflow.

Methods. We obtained new VLT/MUSE WFM and deep NRAO/VLA B-configuration 21 cm data of the galaxy. The MUSE data provide morphology, kinematics, and emission line ratios of Hβ/Hα and [O III]λ5007/Hα of the low surface-brightness filaments, while the VLA data deliver morphology and kinematics of the neutral gas in and around the system. Both datasets are used in concert for comparisons between the ionised and the neutral phase.

Results. We report the prolongation of a lacy filamentary ionised structure up to a projected distance of 16 kpc at $SB_{H\alpha} = 1.5 \times 10^{-18}$ erg s cm^{-2} arcsec^{-2}. The filaments exhibit unusual low Hα/H$\beta \approx 2.4$ and low [O III]/H$\alpha \sim 0.4$–0.6 typical of diffuse ionised gas. They are spectrally narrow (~20 km s^{-1}) and exhibit no velocity sub-structure. The filaments extend outwards from the elongated H I halo. On small scales, the N_{HI} peak is offset from the main star-forming sites. The morphology and kinematics of H I and H II reveal how star-formation-driven feedback interacts differently with the ionised and the neutral phase.

Conclusions. We reason that the filaments are a large-scale manifestation of star-formation- driven feedback, namely limb-brightened edges of a giant outflow cone that protrudes through the halo of this gas-rich system. A simple toy model of such a conical structure is found to be commensurable with the observations.

Key words. galaxies: starburst – galaxies: halos – galaxies: individual: SBS 0335−052E – ISM: jets and outflows

1. Introduction

The response of interstellar gas to energy and momentum deposition from supernovae and stellar winds is the growth of a hot bubble surrounded by a dense shell. Star-forming populations can inject energy and momentum long enough to sweep the shell up and out to lower density gas, where Rayleigh-Taylor instabilities eventually deform it before breaking it up. The hot gas then vents into the circum-galactic halo of the galaxy as a wind that also entrains warm and cold gas. If the wind is powerful enough, the gas may escape the gravitational potential of a galaxy and thereby enrich the intergalactic medium (IGM) with metals. The gas from less powerful outflows then rains back on the galaxy and is available to form the next generation of stars. Outflows and winds – next to inflows of fresh gas – are a cornerstone of galaxy formation models and are vital for regulating cosmic chemical evolution (see reviews by Veilleux et al. 2005, 2020; Collins & Read 2022; as well as Schneider & Robertson 2018; Nelson et al. 2019; Mitchell et al. 2020; Schneider et al. 2020; Pandya et al. 2021 for state-of-the-art computer models).

Observationally, signatures of galactic outflows in star-forming galaxies are ubiquitous, both in the nearby (e.g. Heckman et al. 2011; Chisholm et al. 2016) and in the high-redshift universe (review by Erb 2015). Galaxies in the local Universe allow for detailed panchromatic mappings of outflow phenomena, from the highest energies (cosmic rays and hot gas) to the longest wavelengths possible (cold and molecular gas) – especially if the outflow occurs 'edge-on'. The most detailed observational studies that analyse multiple phases of outflows simultaneously are performed on nearby, more evolved, and massive systems. These observations nourish our

★ Data products are only available at the CDS via anonymous ftp to cdsarc.cds.unistra.fr (130.79.128.5) or via https://cdsarc.cds.unistra.fr/viz-bin/cat/J/A+A/670/A121

A&A 670, A121 (2023)

Outflows: Key process for understanding galaxies.

Star-formation driven feedback and outflows regulate availability and chemical composition of gas for forming stars (in concert with inflows).

Impact

- star-formation history
- size
- colour
- metallicity
- inner dark-matter density profiles
- …

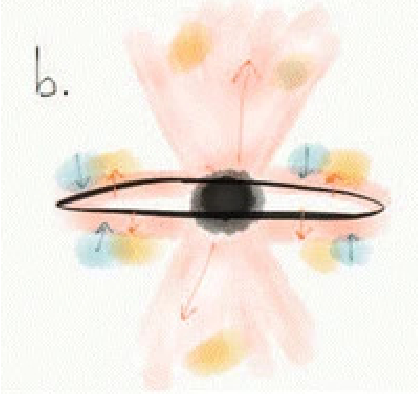

Outflows are important in regulating f_{esc}^{LyC} & $f_{esc}^{Ly\alpha}$

Beamed outflows: LyC/Lyα escape into small solid angles.

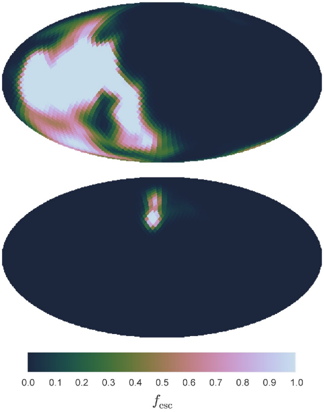

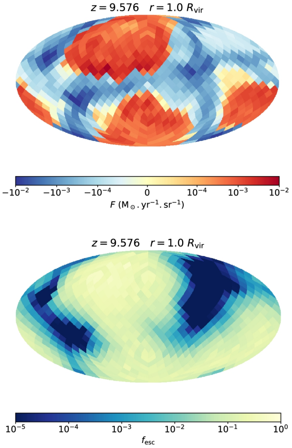

2 massive haloes ($M_H \sim 10^7 M_\odot$) at $z \sim 12$

$M_H \sim 10^8 M_\odot$

Paardekooper et al. (2015)

Trebitsch et al. (2017)

Outflow simulation of an individual galaxy

GPU based - run on Titan super computer - assumes α

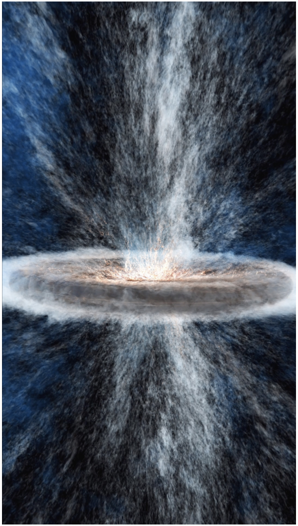

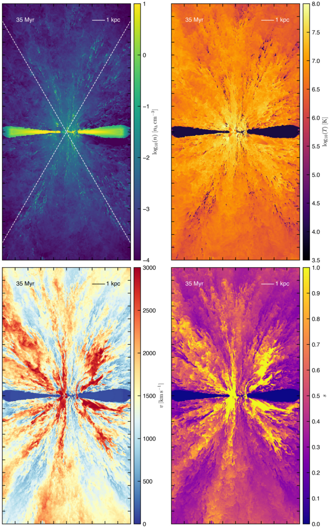

Evan E. Schneider et al 2020 ApJ 895 43

Key quantity to characterise winds: $\eta = \dot{M}_{\rm wind} / \dot{M}_{\rm SFR}$.

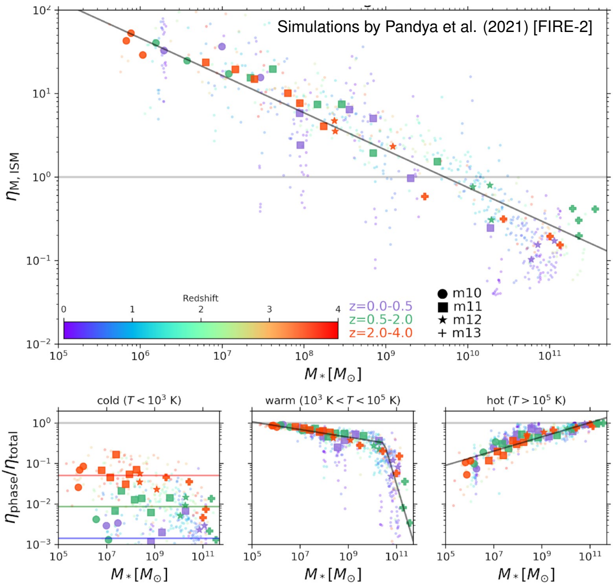

Starburst galaxies: most mass loaded in the warm phase.

Mapping the diffuse ionised gas - Hα

Hα (λ6563) from volume V, density n ($\sim n_e \sim n_p$), temperature T in recombination equilibrium ($E_{\mathrm{ion}} = 1\,\mathrm{Ry}$):

$$L_{\mathrm{H}\alpha} = \epsilon_{\mathrm{H}\alpha}(T) \times n^2 \times V \quad (1)$$

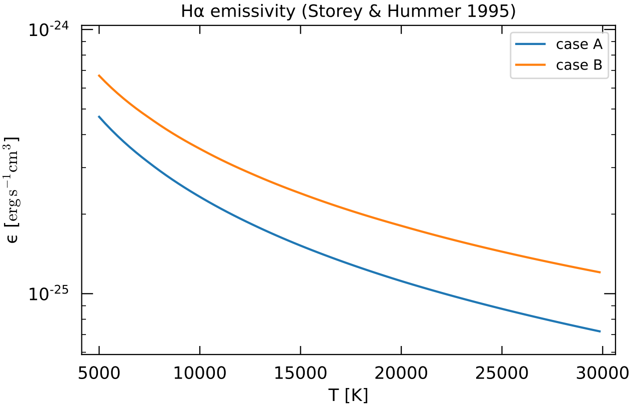

Mapping the diffuse ionised gas - [O III] $\lambda 5007$

Collisional Excitation of O^{2+} ($E_{\rm ion} = 2.58\,\rm Ry$) $\rightarrow$ "Forbidden" Line (magnetic dipole transition).

$$L_{\lambda 5007} = j_{\lambda 5007}(T) \times n_e \times n(\mathrm{O}^{2+}) \times V \qquad (2)$$

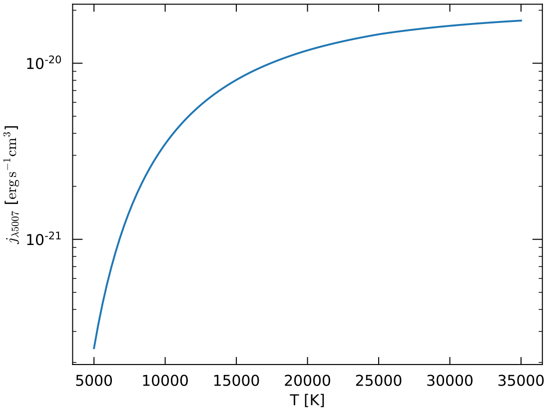

Collisional emissivity from `pyneb` (Luridiana, Morisset & Shaw 2015).

VLT/MUSE – ideal instrument to map outflows spatially

Unprecedented sensitivity for low-SB line emission.

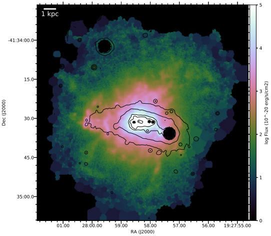

ESO 338 - $d = 40\,\mathrm{Mpc}$
$M_{\mathrm{dyn}} \sim 10^8 \mathrm{M}_\odot$
(Bik et al. 2018)

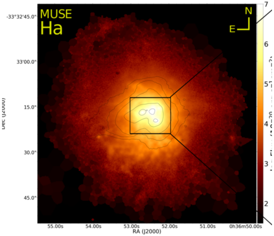

Haro 11 - $d = 87\,\mathrm{Mpc}$
$M_{\mathrm{dyn}} \sim 10^{10\ldots11} \mathrm{M}_\odot$
(Menacho et al. 2019)

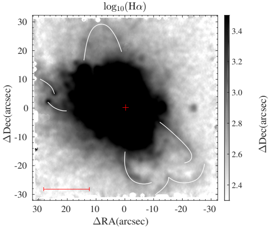

Haro 14 – $d = 13\,\mathrm{Mpc}$
$M_{\mathrm{dyn}} \sim 10^8 \mathrm{M}_\odot$
(Cáiros et al. 2022)

Seems like every star-bursting dwarf observed with MUSE shows extended Hα structures (relative to continuum).

The SBS 0335-052 system ($d = 58$ Mpc / $z = 0.0135$)

A “reference laboratory” for understanding high-z galaxies

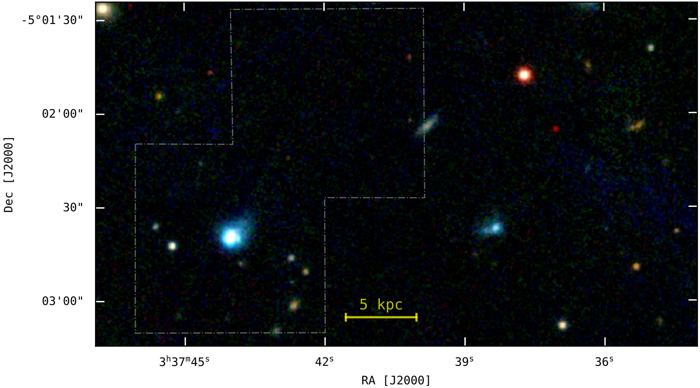

SBS 0335-052E: $\mathrm{M_{UV}} = -16.4$, $M_\star = 5.7 \times 10^6\,\mathrm{M_\odot}$,
$SFR = 1.2\,\mathrm{M_\odot yr^{-1}}$, $12 + \log(\mathrm{O/H}) = 7.25$

Izotov et al. 1990, Nature 343, 238.

(SBS 0335-052W: $12 + \log(\mathrm{O/H}) = 6.86 \ldots 7.22$)

HST: Age Gradient (SE→NW) & Hα super-shell.

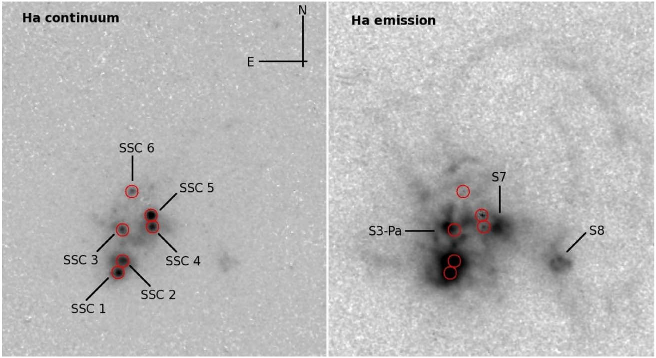

Properties of the Six SSCs. SED at Fixed Age for Mass Determination. Age is Determined Through EW(Hα)

IDs	$f(\mathrm{H}\alpha)$ (erg s^{-1} cm^{-2})	EW (Hα) (Å)	Age (R08)[a] (Myr)	Age[b] (Myr)	Mass ($M_\odot$)	A_V (mag)	$R_{\mathrm{H\,II}}$ (pc)
SSC1	5.14×10^{-14} (1%)	3100.0(134.4)	$\leqslant 3.3$	3.0	4.7×10^5	0.73	11.3(11.5)[c]
SSC2	3.34×10^{-14} (1%)	2300.0(104.7)	$\leqslant 3.4$	3.0	3.7×10^5	0.65	10.4(9.7)[c]
SSC3	5.77×10^{-15} (2.5%)	787.0(53.4)	6.8(2.5)	7.0	7.1×10^5	0.92	29.1(26.6)[d]
SSC4	2.42×10^{-15} (3.9%)	176.0(10.7)	12.4(1.7)	11.0	1.1×10^6	0.20	32.9(26.9)[e]
SSC5	2.29×10^{-15} (4.5%)	84(4.4)	15.1(2.3)	13.0	2.9×10^6	0.84	38.6(29.5)[e]
SSC6	6.34×10^{-16} (7.7%)	187(22.5)	13.9(1.9)	11.0	2.6×10^5	1.08	20.6(21.49)[e]

Reines A.E. et al. 2008, AJ 136, 1415. Adamo A. et al. 2010, ApJ 725, 1620.

Let's zoom out (HST FR565N, F550M, & now MUSE).

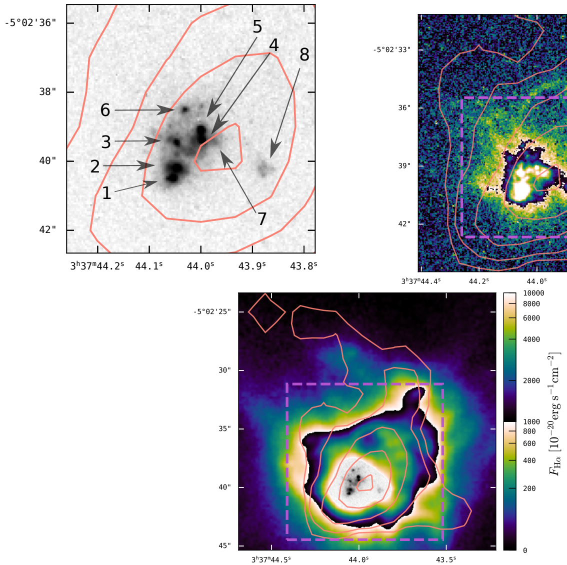

$t_{\mathrm{exp}} \approx 1.5\,\mathrm{h}$

$N_{\mathrm{HI}} = \{5, 10, 20, 30, 40\} \times 10^{20}\mathrm{cm}^{-2}$

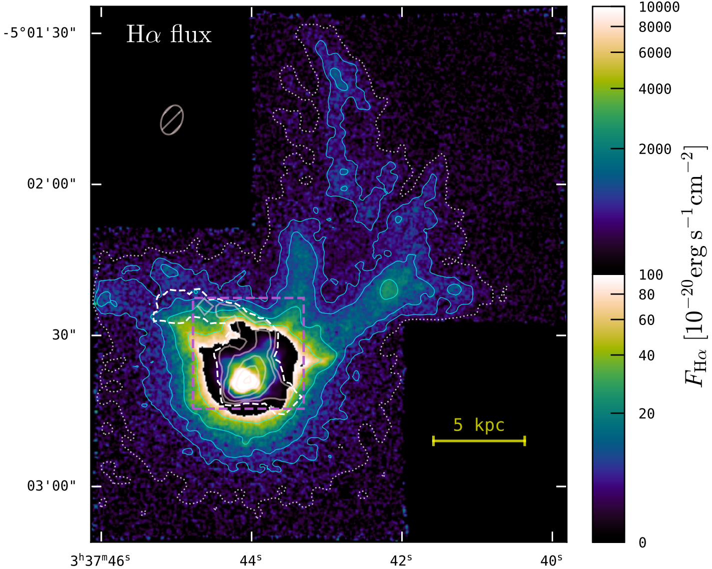

$1'35'' \times 1'46''$ (26.2 kpc × 29.2 kpc).
Contours: $\mathrm{SB}_{\mathrm{H}\alpha} = \{0.75, 1.5, 2.5, 5, 12.5\} \times 10^{-18}\mathrm{erg\,s^{-1}\,cm^{-2}\,arcsec^{-2}}$ (dotted white & cyan),
$N_{\mathrm{HI}} = \{2.5, 5, 10, 20, 30, 40\} \times 10^{20}\mathrm{cm^{-2}}$ (dashed white & grey).

Structure extends outward of HI Halo

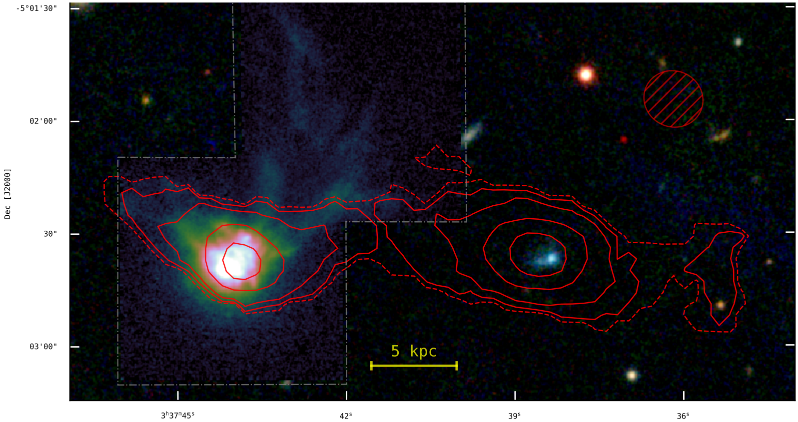

Hα – log-stretch from 0 to $1.25 \times 10^{-15}\,\mathrm{erg\,s^{-1}cm^{-2}}$.

21 cm – contours $N_{\mathrm{HI}} = \{0.5(2.5\sigma), 1, 2, 5, 8\} \times 10^{20}\,\mathrm{cm}^{-2}$.

Background: grz colour composite (Pan-STARRS).

Kinematics of H II

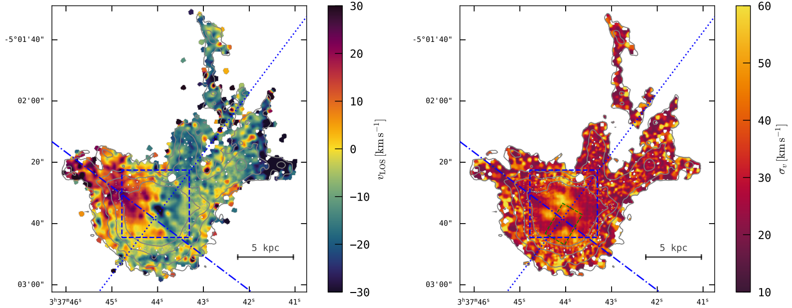

Filaments characterised by:

- Narrow lines – $\sigma_v = 20 \ldots 30\,\mathrm{km\,s^{-1}}$.
- No velocity gradient in outwards direction. Perhaps small $\Delta v \sim 5\,\mathrm{km\,s^{-1}}$ between them.

Symmetric bifurcation wrt. to minor axis. *Clue for outflow.*

MUSE Detections of Hα, Hβ, [O III] λ5007

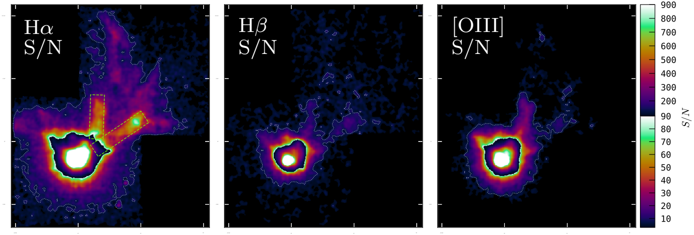

Contour: $SN_{\mathrm{LSD}} = 8$.

S/N after 3D Gaussian filter ($\sigma_v = 150\,\mathrm{km\,s^{-1}}$, $\sigma_{2D} = 2''$)
LSDCat (Herenz, E. & Wisotzki L. 2017),
see also LSDCat2.0 (Herenz 2023, see poster).

Line Ratio Analysis — Hβ/Hα & [O III]/Hα

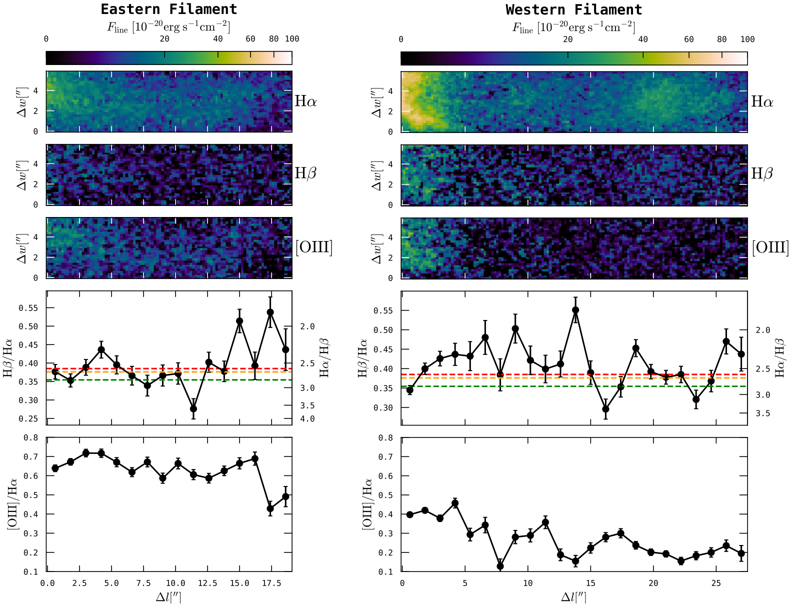

HI vs. HII kinematics

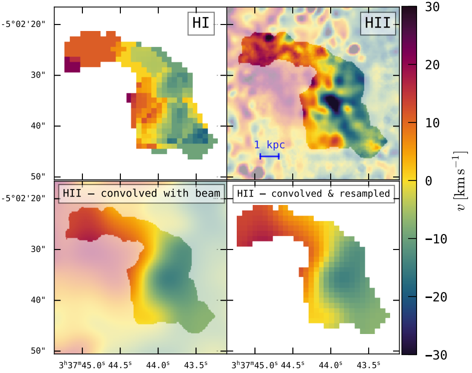

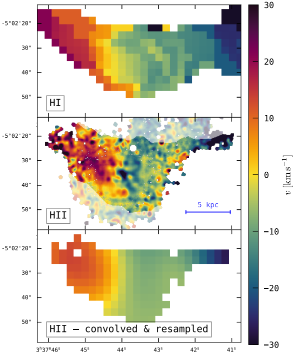

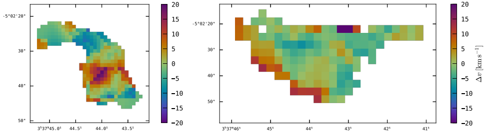

Bulk of H II not comoving with H I.

What are the filaments? Cone-Wall Structure.

Geometrical Parameters: θ (opening angle), ϑ (position angle), i (inclination), h (height), t (wall thickness).

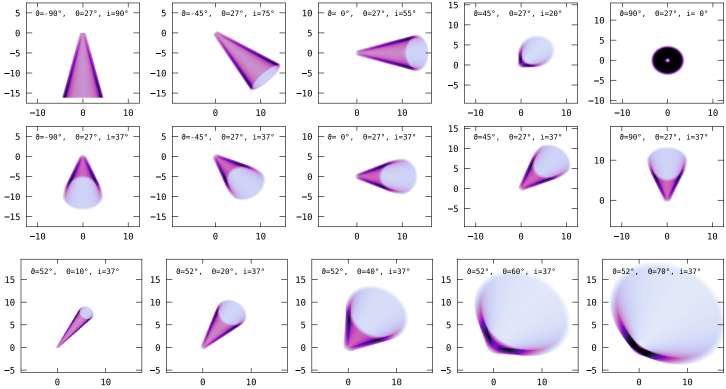

Inside: $V_{\rm hot} = \pi/3 \cdot \tan^2(\theta/2) \cdot h^3$

Walls: $V_{\rm HII} = \pi/3 \cdot \tan^2(\theta/2) \cdot \left((h+\Delta h)^3 - h^3 - \Delta h^3\right)$, with $\Delta h = 2 \cdot t \cdot \cos(\theta/2)$.

Volumes $V_{\rm HII}$ and $V_{\rm hot}$.

Fix geometrical parameters from observations:

- $\vartheta = 52^\circ$, $i = 43^\circ$ (Moiseev et al. 2010).
- $\theta = 2 \times \arctan[\sin(i) \times \tan(\theta_P/2)] = 27^\circ$, where $\theta_P = 34^\circ$ is the observed opening angle.
- $h = l_p \cdot \cos(\theta/2)/\sin(i) = 16.2\,\mathrm{kpc}$, where $l_p = 10\,\mathrm{kpc}$ is the projected length of the filaments.
- $t = 1.5\,\mathrm{kpc}$.

$$\underline{V_{\rm hot} = 256\,\mathrm{kpc}^3} \qquad \underline{V_{\rm HII} = 142\,\mathrm{kpc}^3} \tag{3}$$

Hot phase: Mass, Mass Loading (η), & $v_{\rm wind}$

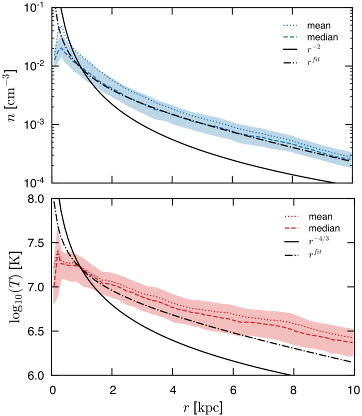

$$M_{\rm hot}(V_{\rm hot}, n) = 6 \times 10^{5\ldots6}\,{\rm M}_\odot.$$

$$\underline{\eta_{\rm hot} \lesssim 0.1}$$

in $M_{\rm hot} = \int \eta_{\rm hot} \dot{M}_\star \, {\rm d}t$ with $\Delta t = 10\,{\rm Myr}$
and $\dot{M}_\star \approx 1 {\rm M}_\odot {\rm yr}^{-1}$

$$v_{\rm wind} = h/(t_* - t_{\rm SN}) = 16.2\,{\rm kpc}/10\,{\rm Myr} = 1620\,{\rm km\,s}^{-1}$$

for $t_* = 15\,{\rm Myr}$ and $t_{\rm SN} = 5\,{\rm Myr}$.

$$T_{\rm hot} \sim 10^6 \ldots 10^7\,{\rm K},$$
$$n \sim 10^{-3} \ldots 10^{-4}\,{\rm cm}^{-3}.$$

(CGOLS; Schneider et al. 2020)

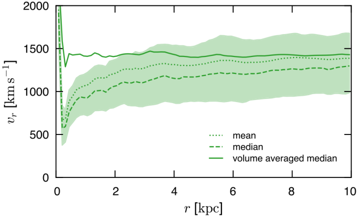

Warm phase: Mass, Mass Loading, Observability

Fix n and T in Eq. (1), such that we reproduce the observed flux $F_{\mathrm{H}\alpha} =$ with V_{HII} from Eq. (3) (assuming Case-A):

$$n = \{3, 4, 5\} \times 10^{-2}\,\mathrm{cm}^{-3} \quad \text{for} \quad T = \{1, 1.5, 2\} \times 10^{4}\,\mathrm{K} \quad (4)$$

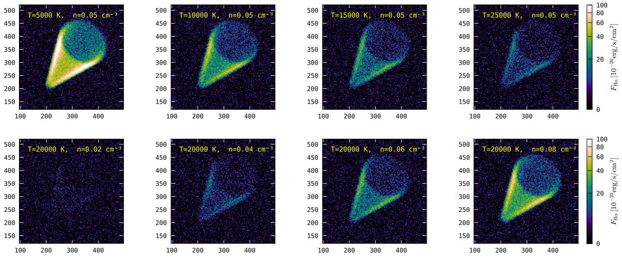

Figure: Simulated MUSE Hα observations of cone-wall structure for varying T and n.

Best match to observations:

$n = 5 \times 10^{-2}\,\mathrm{cm}^{-3}$ & $T = \{1, 1.5, 2\} \times 10^{4}\,\mathrm{K}$

$$\Rightarrow \underline{M_{\mathrm{HII}} = 1.5 - 1.7 \times 10^{8}\,\mathrm{M}_{\odot}} \quad \underline{\eta_{\mathrm{HII}} \gtrsim 10}$$

Toy model consistent with observations and theory

Provides realistic masses and loading factors. Required T and n consistent with expectations for "hot" and "cool" phase of outflow. Reproduces basic H II morphology.

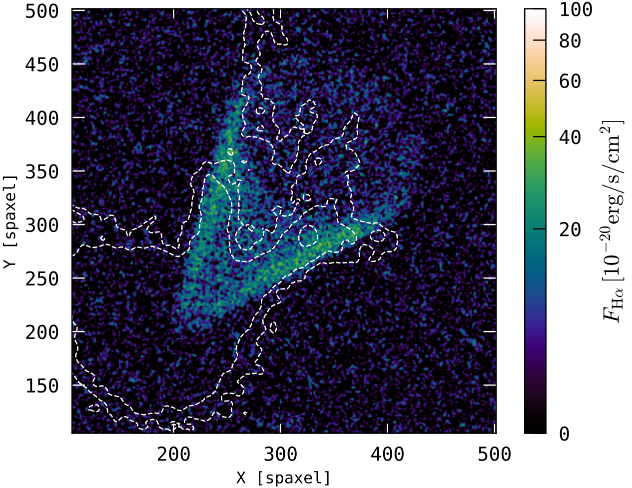

Implications for the Epoch of Reionisation?

Reionisation often conceptualised via “ionised” bubbles.

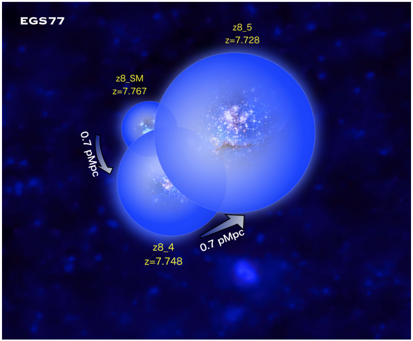

Tilvi et al. (2020, ApJL 891, L10): 3 Lyα emitting galaxies at $z = 7.7$ (Keck/MOSFIRE)

$$R_S = \left(\frac{3 \dot{N}_{\rm ion} f_{\rm esc} t}{4\pi n_{\rm HI}(z)} \right)^{1/3}$$

Evolution of EoR: pre-overlap $\rightarrow$ overlap $\rightarrow$ post-overlap...

EoR is phase transition.

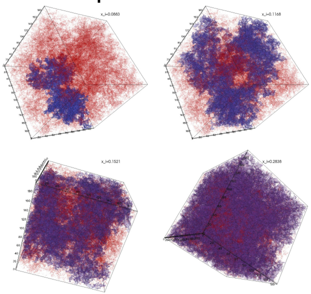

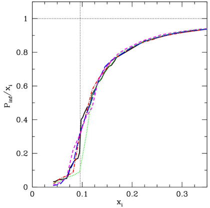

Furlanetto & Oh (2016) - spherical symmetry in those models: *“The overlap phase* – $0.1 \lesssim x_i \lesssim 0.9$ – *sees the ionized and neutral gas almost entirely contained in just two distinct, delicately intertwined regions.”*

Summary on SBS0335-052E

- SBS0335-052E shows two low-SB Hα filaments $\mathrm{SB}_{\mathrm{H}\alpha} \approx 1.5 \ldots 3 \times 10^{-18}$erg s^{-1}cm^{-2}arcsec^{-2}), that extend outside of H I halo.
- Balmer decrement indicative of low optical depth (neither Case-A nor Case-B).
- Direction and symmetry with respect to kinematic model of the galaxy: Clue for Outflow.
- Geometrical toy model reproduces observables, when fed with input parameters (n, T) according to theoretical expectations for the wind.